THE JOURNAL OF BIOLOGICAL CHEMISTRY
Vol. 279, No. 41, Issue of October 8, pp. 43098–43106, 2004
Printed in U.S.A.

Catalase-peroxidases (KatG) Exhibit NADH Oxidase Activity*

Received for publication, June 8, 2004, and in revised form, July 22, 2004
Published, JBC Papers in Press, July 26, 2004, DOI 10.1074/jbc.M406374200

Rahul Singh‡, Ben Wiseman‡, Taweewat Deemagarn‡, Lynda J. Donald§, Harry W. Duckworth§, Xavi Carpena‡, Ignacio Fita¶, and Peter C. Loewen‡‖

From the ‡Department of Microbiology, University of Manitoba, Winnipeg, Manitoba R3T 2N2, Canada, the §Department of Chemistry, University of Manitoba, Winnipeg, Manitoba R3T 2N2, Canada, and the ¶Consejo Superior de Investigacione Cientifícas, Parc Cientific, Josep Samitier 1-5, 08028 Barcelona, Spain

Catalase-peroxidases (KatG) produced by *Burkholderia pseudomallei*, *Escherichia coli*, and *Mycobacterium tuberculosis* catalyze the oxidation of NADH to form NAD^+ and either H_2O_2 or superoxide radical depending on pH. The NADH oxidase reaction requires molecular oxygen, does not require hydrogen peroxide, is not inhibited by superoxide dismutase or catalase, and has a pH optimum of 8.75, clearly differentiating it from the peroxidase and catalase reactions with pH optima of 5.5 and 6.5, respectively, and from the NADH peroxidase-oxidase reaction of horseradish peroxidase. *B. pseudomallei* KatG has a relatively high affinity for NADH (K_m = 12 μM), but the oxidase reaction is slow (k_{cat} = 0.54 min^{-1}) compared with the peroxidase and catalase reactions. The catalase-peroxidases also catalyze the hydrazinolysis of isonicotinic acid hydrazide (INH) in an oxygen- and H_2O_2-independent reaction, and KatG-dependent radical generation from a mixture of NADH and INH is two to three times faster than the combined rates of separate reactions with NADH and INH alone. The major products from the coupled reaction, identified by high pressure liquid chromatography fractionation and mass spectrometry, are NAD^+ and isonicotinoyl-NAD, the activated form of isoniazid that inhibits mycolic acid synthesis in *M. tuberculosis*. Isonicotinoyl-NAD synthesis from a mixture of NAD^+ and INH is KatG-dependent and is activated by manganese ion. *M. tuberculosis* KatG catalyzes isonicotinoyl-NAD formation from NAD^+ and INH more efficiently than *B. pseudomallei* KatG.

Isonicotinic acid hydrazide (isoniazid or INH)[1] is a widely used pro-drug effective against *Mycobacterium tuberculosis* (Ref. 1 and other reviews therein). Formation of isonicotinoyl-NAD, the active form of the drug, involves removal of hydrazine from INH by KatG (2) and ligation of the isonicotinoyl group with NAD^+ (3). Isonicotinoyl-NAD interferes with the synthesis of mycolic acid and therefore cell wall synthesis by binding to InhA, an enoyl-acyl carrier protein reductase (4), and possibly to KasA, a β-ketoacyl acyl carrier protein synthase (5), blocking their NADH-binding sites. The central role of KatG in INH activation is evident in the significant fraction of INH-resistant cases of tuberculosis attributable to mutations in *katG* and in biochemical studies that have demonstrated a direct role for KatG in the generation of various isonicotinoyl derivatives (6). Much of the literature related to the activation of INH by KatG has focused on the fate of INH and possible intermediates involved in the process (6–8). With NAD^+ included in the mix, the generation of the isonicotinoyl-NAD adduct was observed both with and without KatG present (7–9), leading to the suggestions that the role of KatG is limited to the hydrazinolysis of INH and that the subsequent reaction of the isonicotinoyl radical with NAD^+ is a nonenzymatic event involving a homolytic aromatic substitution (7, 10). Reactive oxygen species have been implicated in INH activation both *in vivo* (11, 12) and *in vitro* (6), and an elevated level of superoxide (13) was identified as a possible reason for the high sensitivity of *M. tuberculosis* to INH (1). However, the absence of H_2O_2 involvement in INH activation implies that a reaction different from either the peroxidase or the catalase reactions is involved, and some reports have suggested that the active participation of KatG in INH activation involves more than just hydrazinolysis (9).

NADH oxidases are widely distributed in nature, being found in species ranging from bacteria (14, 15) and archaebacteria (16) to mammals (17). The enzyme can be both soluble and membrane-bound, and although NADH is the common electron donor, water, hydrogen peroxide, or superoxide may be formed as products depending on the enzyme. The physiological role of NADH oxidases in many instances is unknown, but the reaction has been described as a detoxifier of oxygen in nitrogen fixing organisms and archaebacteria (16) and as a possible sensor of oxygen levels in the regulation of muscle contractility (17). A variation of the NADH oxidase reaction, a "peroxidase-oxidase" reaction has been well characterized in horseradish peroxidase (HRP) to require a catalytic amount of H_2O_2 that is alternately used and regenerated during the reaction of NAD radicals with molecular oxygen (Refs. 18–20 and reviewed in Ref. 21). Plant peroxidases, including HRP, have about 20% sequence similarity and remarkable structural similarity to the N-terminal domain of KatG proteins, particularly in the vicinity of the heme active site, raising the possibility that KatG proteins may also exhibit an NADH peroxidase-oxidase activity. Indeed, there are reports of NADH being oxidized to NAD^+ by KatG in both peroxidase (22) and an oxidase-like (7) reactions, but the reaction of KatG with NADH has not been characterized. Given the potential importance of any reaction involving NADH in isonicotinoyl-NAD formation, this report investigates the interactions of KatG with NADH, demonstrat-

* This work was supported by Grant OGP9600 from the Natural Sciences and Engineering Research Council of Canada (to P. C. L.), by the Canadian Research Chair Program (to P. C. L.), and by Fellowship EX-2003-0866 from the Ministerio de Educación Cultura y Deporte, Spain (to X. C.). The costs of publication of this article were defrayed in part by the payment of page charges. This article must therefore be hereby marked "*advertisement*" in accordance with 18 U.S.C. Section 1734 solely to indicate this fact.

‖ To whom correspondence should be addressed: Dept. of Microbiology, University of Manitoba, Winnipeg, MB R3T 2N2, Canada. Tel.: 204-474-8334; Fax: 204-474-7603; E-mail: peter_loewen@umanitoba.ca.

[1] The abbreviations used are: INH, isonicotinic acid hydrazide; HRP, horseradish peroxidase; ABTS, 2,2′-azinobis(3-ethylbenzothiazolinesulfonic acid); NBT, nitroblue tetrazolium; HPLC, high pressure liquid chromatography; CHES, 2-(cyclohexylamino)ethanesulfonic acid.

ing an oxygen-dependent NADH oxidase activity and a direct role for KatG in the formation of isonicotinoyl-NAD.

EXPERIMENTAL PROCEDURES

Strains and Plasmids—The plasmids pAH1 (23), pBpKatG (24), and pBT22 (25) were used as the source of catalase-peroxidases from *M. tuberculosis*, *Burkholderia pseudomallei*, and *Escherichia coli*, respectively. All of the plasmids were transformed into the catalase-deficient *E. coli* strain UM262 (*pro leu rpsL hsdM hsdR endI lacY katE1 katG17*::Tn10 *recA*) (26) and grown in Luria broth containing 10 g/liter tryptone, 5 g/liter yeast extract, and 5 g/liter NaCl for expression of the catalase-peroxidases. Subsequent purification of the enzymes was essentially as described (24).

Enzyme and Protein Determination—Catalase activity was determined by the method of Rorth and Jensen (27) in a Gilson oxygraph equipped with a Clark electrode. One unit of catalase is defined as the amount that decomposes 1 μmol of H_2O_2 in 1 min in a 60 mM H_2O_2 solution at pH 7.0 at 37 °C. Peroxidase activity was determined spectrophotometrically using ABTS (28). One unit of peroxidase is defined as the amount that decomposes 1 μmol of ABTS in 1 min in a solution of 0.3 mM ABTS (ϵ = 36,800 M^{-1} cm^{-1}) and 2.5 mM H_2O_2 at pH 4.5 and 25 °C. The peroxidatic substrate *o*-dianisidine was also tested, but the data are not reported. Free radical production was assayed by nitroblue tetrazolium (NBT) reduction to a monoformazan (ϵ = 15,000 M^{-1} cm^{-1}). NADH oxidase activity was determined spectrophotometrically at 340 nm using ϵ = 6,300 m^{-1} cm^{-1} for NADH. One unit of NADH oxidase is defined as the amount that produces 1 nmol of radical or that decomposes 1 nmol of NADH in a solution of 250 μM NADH at 25 °C. The protein was estimated according to the methods outlined by Layne (29).

Polyacrylamide Gel Electrophoresis and Visualization of Enzymatic Activities—Gel electrophoresis of purified proteins was carried out under denaturing conditions on SDS-polyacrylamide gels as previously described (30, 31). Gel electrophoresis was carried out under nondenaturing conditions according to Davis (32), except in pH 8.1 Tris-HCl. Following electrophoresis, peroxidase activity was visualized by the method of Gregory and Fridovich (33), and catalase was visualized as described by Clare *et al.* (34), but using 20 mM H_2O_2 for better contrast. KatG mediated oxidation of INH and NADH was visualized using NBT as described by Hillar and Loewen (23).

Mass Spectrometry—BpKatG was dialyzed into 5 mM ammonium acetate, and NADH was dialyzed against three changes of 1 liter 0.1 M ammonium bicarbonate, after which the concentration was determined by A_{340}. The matrix solution was freshly prepared each day at 160 mg/ml 2,5-dihydroxybenzoic acid in 3:1 water:acetonitrile, 2% formic acid solution. 20-μl reaction mixtures contained 200 μg/ml BpKatG, 128 μM NADH, and 10 mM INH in 0.1 M NH_4HCO_3 at room temperature. 0.5-μl aliquots were removed at 1 min, 2 h, 4 h, and 18 h and immediately mixed with 0.5 μl of matrix solution on a metal target. The samples were analyzed on a QqTOF mass spectrometer (35).

Determination of Conserved Residue Locations—The locations of residues conserved in >95% of 52 available KatG sequences were determined using the program CONRES. The program identifies conserved residues in an alignment file from CLUSTALW (36) and extracts the equivalent residues from the structure of one of the aligned proteins. The sequence alignment file included 52 catalase-peroxidase sequences and the structure file for *B. pseudomallei* KatG (Protein Data Bank code 1MWV) was used as the model. The accession numbers for the sequences included in the comparison are listed by Klotz and Loewen (37). The source code or IRIX 6.5 executable for CONRES can be obtained from the authors on request.

RESULTS

NADH Oxidation by KatG—NAD^+ replaces the hydrazine moiety of the anti-tubercular pro-drug INH to generate the active form of the drug, isonicotinoyl-NAD. In an attempt to define more precisely the role of KatG in the formation of isonicotinoyl-NAD, the potential utilization of NADH and NAD^+ as substrates was investigated, revealing that NADH supports BpKatG-mediated radical generation (Fig. 1*a*) in the absence of H_2O_2 using NBT as radical sensor at a rate approximately equal to the rate of NADH disappearance (Fig. 1*b*). NADPH supports a slower rate of radical generation, and NAD^+ does not support any radical production (Table I). NAD^+ was confirmed as the product of the reaction with NADH by HPLC analysis (Fig. 2). Both superoxide dismutase and a lower

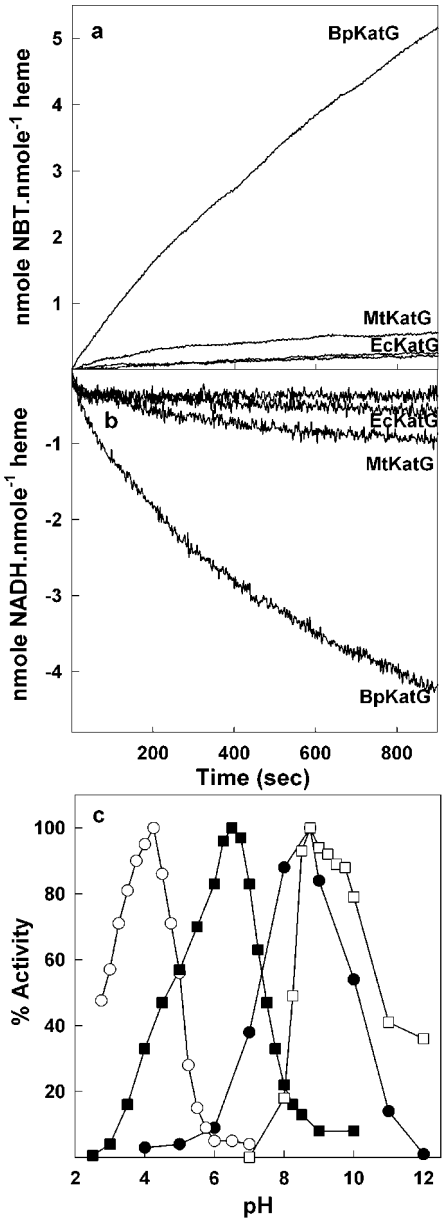

FIG. 1. **NADH oxidation by catalase-peroxidases.** *a*, the rates of radical production in a solution containing 100 μM NADH, 1.2 μM enzyme, 200 μM NBT, and 50 mM Tris, pH 8.75, are followed by formazan appearance measured at 560 nm. Separate assays contain no enzyme (control), BpKatG, MtKatG, or EcKatG. *b*, the rates of NADH oxidation in a solution containing 100 μM NADH, 1.2 μM enzyme, and 50 mM Tris, pH 8.75, was followed by NADH disappearance measured at 340 nm. Separate assays contain no enzyme (control), BpKatG, MtKatG, or EcKatG. *c*, pH dependence of NADH oxidation by BpKatG determined by radical formation at 560 nm (□) and NADH disappearance at 340 nm (●) compared with the pH dependence of the catalase (■) and peroxidase reactions (○). Buffered solutions contained 50 mM each of sodium acetate, pH 3, 4, and 5; potassium phosphate, pH 6 and 7; Tris-HCl, pH 8 and 9; and CHES, pH 10.

molecular oxygen concentration reduce radical generation (Table I) from NADH. The pH optima for both radical production and NADH disappearance are 8.75, but the curves are not perfectly superimposable (Fig. 1*c*), suggesting two different, pH-dependent, fates for the reduced oxygen, most likely H_2O_2 at lower pH and superoxide radical at higher pH. Unfortunately, the rapid degradation of H_2O_2 by both the catalase and peroxidase activities of BpKatG precluded its identification or even the observation of any spectral changes in the enzyme

TABLE I
BpKatG-mediated radical production in the presence of different substrates

	No enzyme[a]	BpKatG[b]	MtKatG[b]	EcKatG[b]
	pmol/min	*pmol/min/nmol*	*pmol/min/nmol*	
NADH	3.0 ± 0.2	640 ± 96	100 ± 15	13 ± 4
NADH + Mn^{2+}	2.0 ± 0.1	540 ± 23	99 ± 4	10 ± 4
NADH- O_2[c]	1.0 ± 0.2	320 ± 15	9 ± 2	7 ± 2
NADH + SOD	1.0 ± 0.1	350 ± 8	58 ± 6	5 ± 2
NADPH	1.0 ± 0.1	260 ± 2	1.0 ± 0.1	1.0 ± 0.1
NAD^+	3.0 ± 0.6	ND[d]	ND	ND
NADH + INH	8.0 ± 2	1140 ± 76	260 ± 21	100 ± 6
NADH + INH + Mn^{2+}	290 ± 16	2940 ± 29	830 ± 21	930 ± 91
NAD^+ + INH	4.0 ± 0.3	82 ± 1	79 ± 17	74 ± 19
NAD^+ + INH + Mn^{2+}	140 ± 4	230 ± 12	340 ± 8	220 ± 9
INH	5.0 ± 0.2	76 ± 2	78 ± 5	38 ± 2
INH + Mn^{2+}	190 ± 18	410 ± 3	460 ± 9	450 ± 2
INH - O_2[c]	6.0 ± 2	75 ± 5	78 ± 5	40 ± 3
INH + SOD	5.2 ± 1	90 ± 2	65 ± 5	38 ± 3
INH + pyridoxine	4.0 ± 1	9.0 ± 2	20 ± 5	18 ± 3

[a] All of the reactions contained 200 μM NBT in 50 mM Tris, pH 8.75, supplemented with 10 mM INH, 250 μM NADH, 250 μM NADPH, 250 μM NAD^+, and 200 μg of superoxide dismutase as indicated. O_2 was reduced by flushing the reaction mixture with N_2 gas.
[b] KatG was added to 1.2 μM.
[c] For anaerobic reactions, the reaction mixtures were flushed with nitrogen to remove dissolve oxygen.
[d] ND, not detected.

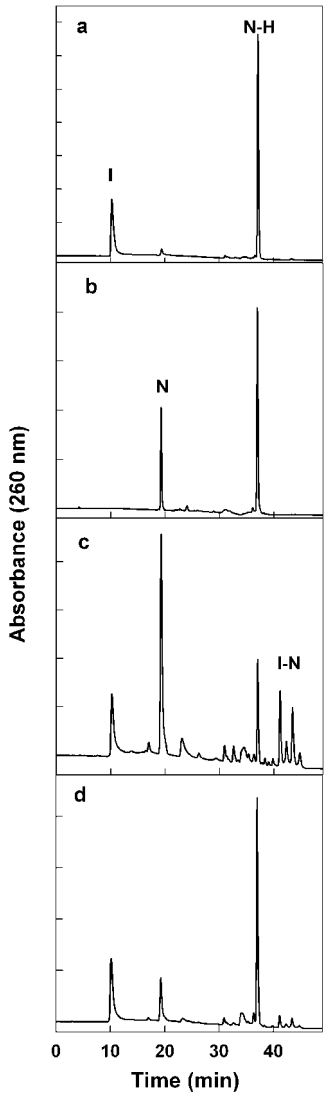

FIG. 2. **Elution profiles from reverse phase HPLC of reaction products from mixtures containing 100 μM NADH and 200 μM INH (*a*); 1.2 μM BpKatG and 100 μM NADH (*b*); 1.2 μM BpKatG, 100 μM NADH, and 200 μM INH (*c*); or 1.2 μM MtKatG, 100 μM NADH and 200 μM INH (*d*).** *I*, isonicotinic acid hydrazide; *N-H*, NADH; *I-N*, isonicotinoyl-NAD.

during the reaction. The optimum pH for the oxidase reaction is significantly different from the optimum pH levels for the peroxidase (pH 4.5) and catalase (pH 6.5) reactions (Fig. 1*c*). These results are consistent with BpKatG having an NADH oxidase activity producing NAD^+ and either superoxide ion or H_2O_2 and with a similar activity existing in MtKatG and EcKatG but at a much lower level.

The kinetic parameters of the BpKatG-mediated NADH oxidase reaction (Table II) reveal a relatively high affinity for NADH but a very slow turnover rate in comparison with the catalase and peroxidase reactions. NAD^+ and pyridoxine act as competitive inhibitors of the NADH oxidase reaction (data not shown). Purified BpKatG migrates as a single band (apparent mass of 78 kDa) on denaturing gels (Fig. 3, *lane a*) with only a small amount of slower migrating dimer. On a nondenaturing gel (Fig. 3, *lanes b–g*), catalase, peroxidase, and oxidase activities all co-migrate with the main bands of protein (*lanes b–e*). The presence of two bands of catalase-peroxidase with the same mass on nondenaturing gels has been noted previously but not explained.

HRP catalyzes an unusual NADH peroxidase-oxidase reaction in which H_2O_2 is required to initiate the reaction, after which there is a cycling of $O_2^{\cdot-}$, H_2O_2, and compound III (reviewed in Ref. 21). Given the sequence similarity between plant peroxidases and catalase-peroxidases, particularly in the active site, the possibility that the NADH oxidase activity of KatG is similar to the peroxidase-oxidase reaction was investigated (Table III). The HRP peroxidase-oxidase reaction is characterized by a need for a catalytic amount of H_2O_2, by inhibition by SOD or catalase, and by long lag periods in the presence of low [NADH] and high [HRP]. NADH oxidation by BpKatG does not exhibit any of these characteristics (Table III). For comparison, NADH oxidation by the W111F variant, which lacks catalase activity, is reduced slightly by catalase, but not SOD, and is significantly enhanced by added H_2O_2, attributable to NADH serving as a peroxidatic substrate. No lag in the initiation of NADH oxidation was evident over a broad range of NADH concentrations or enzyme concentrations for either BpKatG or the W111F variant.

INH Hydrazinolysis by BpKatG—The activation of INH as an anti-tubercular drug by catalase-peroxidases involves removal of the hydrazine moiety and proceeds via a radical producing reaction that can be monitored using NBT as a radical sensor (23). The H_2O_2 independence (Fig. 4*a*) and enhanced

TABLE II
Kinetic constants for enzymatic activities associated with BpKatG

	V_{max}	K_m	k_{cat}	k_{cat}/K_m
	$\mu mol \cdot min^{-1}\ \mu mol \cdot heme^{-1}$	μM[a]	s^{-1}	$M^{-1} \cdot s^{-1}$
Oxidase (ΔA_{340})	$540 \pm 96 \times 10^{-3}$	12.5 ± 2.0	$9.0 \pm 0.4 \times 10^{-3}$	7.2×10^{2}
Peroxidase	1083 ± 29	330 ± 30	10.1 ± 0.27	3.1×10^{4}
Catalase	$902 \pm 20 \times 10^{3}$	7700 ± 400	$8.4 \pm 0.2 \times 10^{3}$	1.1×10^{6}

[a] [NADH] for the oxidase reaction, [ABTS] for the peroxidase reaction, and [H_2O_2] for the catalase reactions.

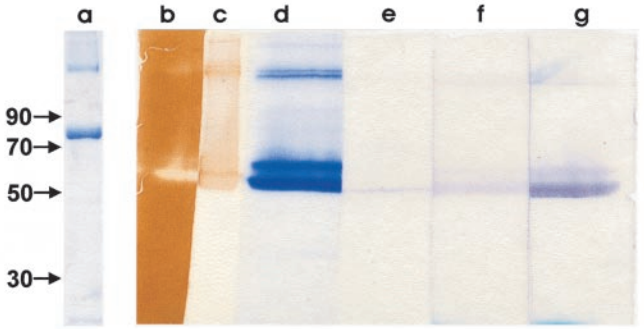

FIG. 3. **Migration of purified BpKatG on a 8% SDS-polyacrylamide gel (*lane a*) and a nondenaturing 8% polyacrylamide gel (*lanes b–g*).** *Lane a* (SDS-polyacrylamide gel) was stained with Coomassie Brilliant Blue dye. A single 200-μg amount of BpKatG was loaded in one large lane for *lanes b–g*, and after electrophoresis, the gel was cut into six strips for separate staining. *Lane b* was stained for catalase activity (a *clear band* on a *brown background*). *Lane c* was stained for peroxidase activity (*brown bands* on a *clear background*). *Lane d* was stained with Coomassie Brilliant Blue. *Lane e* was stained for oxidase activity in a mixture of 200 μM NADH and 200 μM NBT. *Lane f* was stained for INH hydrazinolysis activity in a mixture of 10 mM INH and 200 μM NBT. *Lane g* was stained for combined INH hydrazinolysis and NADH oxidase activity in a mixture of 10 mM INH, 200 μM NADH, and 200 μM NBT.

TABLE III
Comparison of NADH oxidation by HRP, BpKatG, and the W111F variant

All of the reactions contained 100 μM NADH and 100 μg/ml protein in 50 mM Tris, pH 8.75.

	HRP	BpKatG	W111F
NADH	110 ± 18[a]	490 ± 16	500 ± 41
NADH + H_2O_2	360 ± 22	490 ± 24	2160 ± 180
NADH + HPII	30 ± 4	480 ± 16	392 ± 16
NADH + HPII + H_2O_2	54 ± 4	480 ± 16	290 ± 16
NADH + SOD	86 ± 16	400 ± 24	460 ± 16
NADH + SOD + H_2O_2	540 ± 29	400 ± 16	2200 ± 190

[a] The data are expressed as $pmol \cdot min^{-1} \cdot nmol^{-1}$ heme.

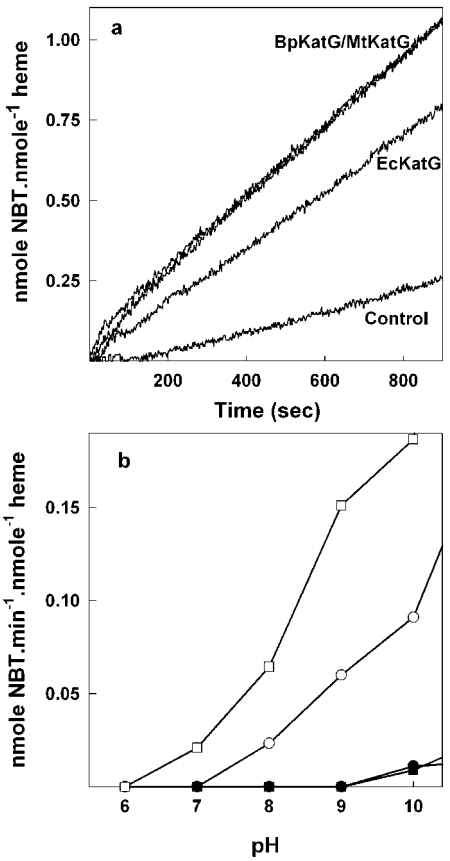

FIG. 4. **Removal of hydrazine from isoniazid.** *a*, radical generation in a solution containing 10 mM INH, 200 μM NBT as radical sensor in 50 mM Tris, pH 8.0, was followed by formazan appearance measured at 560 nm. Separate assays contain no enzyme (control), BpKatG, MtKatG, or EcKatG. *b*, pH dependence of radical generation in a solution of 200 μM NBT with (■) and without BpKatG (●), and a solution of 200 μNBT and 10 mM INH with (□) and without BpKatG (○) is shown.

rates at alkaline pH (Fig. 4*b*) of the KatG-mediated INH hydrazinolysis reaction differentiate it from the catalase and peroxidase reactions (Fig. 1*c*). There is a pH-dependent, nonenzymatic generation of radicals from INH, but in the pH 7–9 range, the contribution of the enzymatic reaction is clear and suggests a pH optimum between 8 and 9, albeit not well defined (Fig. 4*b*). To minimize the nonenzymatic contribution, all subsequent assays and reactions involving INH were carried out at pH 8. Oxygen levels do not affect the KatG-mediated radical generation from INH, and superoxide dismutase does not reduce radical production (Table I), confirming that molecular oxygen does not have a role in the reaction. MtKatG catalyzes INH hydrazinolysis at about the same rate as BpKatG, but the EcKatG-mediated reaction is slower (Fig. 1 and Table I). Despite having a pyridine ring as part of its structure, NAD^+ does not inhibit INH hydrazinolysis (data not shown).

Interaction of KatG with a Mixture of INH and NADH—Radical generation in a mixture of BpKatG, INH, and NADH is about two times faster than the cumulative rate of the individual reactions of INH and NADH (Fig. 5*a*). This rate is further enhanced by the inclusion of 2 μM manganese ion (either Mn^{+2} or Mn^{+3}) (Fig. 5*b*). The rate of NADH disappearance, as measured by the decrease in A_{340}, is similarly increased (data not shown). NAD^+ is not a substrate for radical generation, and the rate of radical formation from a mixture of NAD^+ and INH is the same as with INH alone (Fig. 4*a*) and is enhanced by Mn^{+2} (Fig. 5*c*). The MtKatG- and EcKatG-mediated reactions of INH and NADH are both slower in the absence of Mn^{+2} (Fig. 4*a*) but approach or exceed the BpKatG-mediated reaction in the presence of Mn^{+2} (Fig. 5*b*).

Based on HPLC retention times (Fig. 2) combined with mass spectrometry and tandem mass spectrometry analysis (data not shown), the main products of the combined NADH and INH reaction with KatG are NAD^+ and isonicotinoyl-NAD with other products being present in smaller amounts. Isonicotinoyl-NAD elutes from the column as four peaks, all exhibiting an ion at *m/z* 771, consistent with the report of Wilming and Johnsson (7), who explained the elution pattern as the result of two

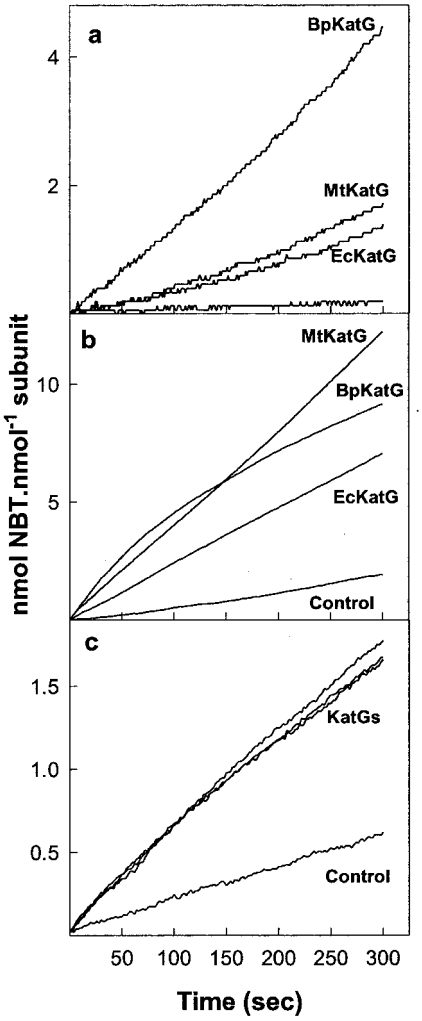

FIG. 5. **Radical generation in a mixture of INH and either NADH (*a* and *b*) or NAD^+ (*c*) mediated by catalase-peroxidases using NBT as radical sensor.** The initial rates of radical production are followed for BpKatG, MtKatG, EcKatG, and no enzyme (control). *a*, the mixture contained 1.2 μM enzyme, 10 mM INH, and 100 μM NADH. *b*, the mixture was as in *a* but with 2 μM Mn^{+2} added. *c*, the mixture contained 200 μM INH, 250 μM NAD^+, and 2 μM Mn^{+2}. Separate assays contain no enzyme (control), BpKatG, MtKatG, or EcKatG.

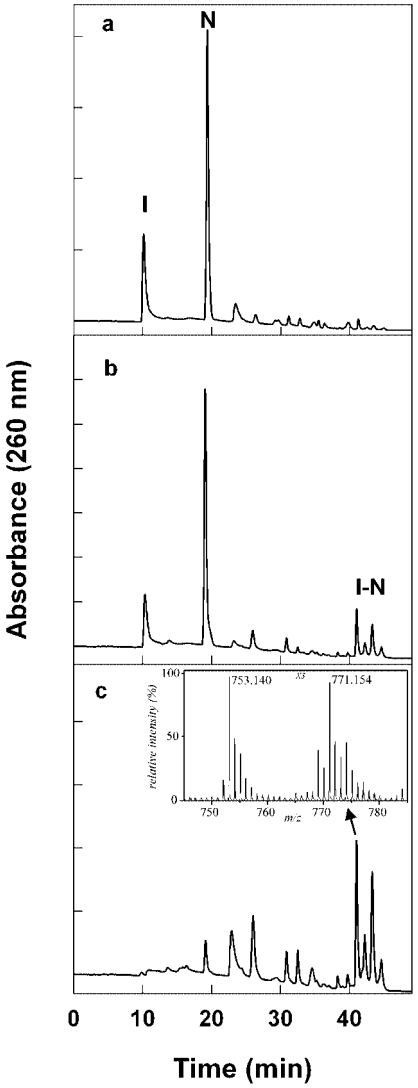

FIG. 6. **Elution profiles from reverse phase HPLC of reaction products from mixtures of 100 μm NAD^+, 200 μM INH, and 2 μM Mn^{2+} (*a*); 1.2 μM BpKatG, 100 μM NAD^+, 200 μM INH and 2 μM Mn^{2+} (*b*); and 1.2 μM MtKatG, 100 μM NAD^+, 200 μM INH, and 2 μM Mn^{2+} (*c*).** The *inset* in *c* shows part of a matrix-assisted laser desorption ionization mass spectrum of a reaction mixture after 18 h of incubation showing the isonicotinoyl-NAD product ion at *m/z* 771 and the decay product at *m/z* 753. *N*, NAD^+; *I-N*, isonicotinoyl-NAD.

stereoisomers, arising from the addition of the isonicotinoyl group to opposite faces of the nicotinamide ring, each with two rotamers, resulting from restricted rotation of the isonicotinoyl group. The time course of appearance and identity of isonicotinoyl-NAD were confirmed by mass spectrometry analysis of the reaction mixture, and the product ion at *m/z* 771 (*inset* to Fig. 6*c*), coincident with the mass of isonicotinoyl-NAD, was evident only in mixtures containing all three of KatG, INH, and NADH or NAD^+. Tandem mass spectrometry measurements of the ions at *m/z* 753 and 771 produced almost identical fragmentation patterns, confirming that the ion at *m/z* 753 is a product of the parent ion at *m/z* 771 (Table IV). The difference in mass between the two ions, 18.014 Da, suggests the loss of H_2O (18.016 Da) but offers no clue as to the structural basis for the decay or its cause. Comparison with the fragmentation pattern of NADH clearly confirms the presence of NAD in the pattern of fragments from the *m/z* 771 and 753 ions (Table IV) degraded from the nicotinamide end and by inference allowing for the isonicotinoyl group, also after degradation from the adenine end (Table IV).

NAD^+ as Precursor for Isonicotinoyl-NAD—The facile KatG-mediated oxidation of NADH and lack of apparent reaction with NAD^+ initially suggested that NADH, not NAD^+, is the precursor to isonicotinoyl-NAD. However, isonicotinoyl-NAD is formed in a KatG-mediated reaction more efficiently from a mixture of NAD^+ and INH (Fig. 6) than from a mixture of NADH and INH, both with 2 μM Mn^{+2} (Fig. 2). Therefore, NAD^+ is the probable precursor for isonicotinoyl-NAD as concluded earlier (7), but NADH oxidation by KatG to NAD^+ will lead to the same product in an NADH mixture. The presence of 2 μM Mn^{+2} greatly speeds the NAD^+-dependent formation of isonicotinoyl-NAD by all three KatGs: BpKatG, MtKatG, and EcKatG.

NADH Oxidation Can Be Uncoupled from Superoxide Formation—It has been well documented that changing any one of a number of residues in KatG reduces catalase activity with minimal effect on peroxidase activity (38–42). A number of variants of BpKatG with residues changed in the active site cavity and in the Met-Tyr-Trp cross-linked structure (43, 44) were assayed for oxidase and hydrazinolysis activities for comparison with their catalase and peroxidase activities (Table V). The hydrazinolysis reaction was largely unaffected by any of the changes except the change of His^{112} to Ala. By contrast, the

TABLE IV
Comparison of expected and observed m/z values of ions in the MS/MS spectra of NADH and the product of the reaction of KatG with INH and NADH identified as isonicotinoyl-NAD

	Product ions (*m/z*) from parent ion[a]			Assigned structure[b]	Formula to calculate expected ion	Expected *m/z*
	m/z 771	*m/z* 753	*m/z* 666			
Parent ions	771.154			IN-NRPPA	$C_{27}H_{33}N_8O_{15}P_2$	771.154
	753.140	753.166		IN-NRPPA-H_2O	$C_{27}H_{31}N_8O_{14}P_2$	753.144
			666.090	NHRPPA (NADH)	$C_{21}H_{30}N_7O_{14}P_2$	666.133
Fragmentation from the adenine end ("y" ions)			530.061	NHRPPR	$C_{16}H_{24}N_2O_{14}P_2$	530.070
			514.059	NHRPPR-NH_3	$C_{16}H_{22}NO_{14}P_2$	514.052
	424.093	424.101		IN-NRP	$C_{17}H_{19}N_3O_8P$	424.091
			319.073	NHRP	$C_{11}H_{16}N_2O_7P$	319.070
	229.044			IN-N	$C_{12}H_{10}N_3O_2$	229.085
			123.063	NH	$C_6H_7N_2O$	123.056
Fragmentation from the nicotinamide end ("b" ions)			649.109	NHRPPA-NH_3	$C_{21}H_{27}N_6O_{14}P_2$	649.106
	664.126			NRPPA	$C_{21}H_{28}N_7O_{14}P_2$	664.117
	542.078	542.072	542.082	RPPA	$C_{15}H_{22}N_5O_{13}P_2$	542.069
	524.059	524.067	524.067	RPPA-H_2O	$C_{15}H_{20}N_5O_{12}P_2$	524.058
	428.041	428.023	428.040	PPA	$C_{10}H_{16}N_5O_{10}P_2$	428.037
	348.073	348.070	348.071	PA	$C_{10}H_{15}N_5O_7P$	348.071
	250.094	250.087	250.100	A	$C_{10}H_{12}N_5O_3$	250.094
	136.070	136.065	136.064	Adenine	$C_5H_6N_5$	136.062

[a] The parent ions at *m/z* 771.154, 753.166, and 666.090 were selected individually and fragmented by tandem mass spectrometry.
[b] A, adenosine; N, nicotinamide; IN, isonicinoyl group; R, ribose.

TABLE V
Comparison of catalase, peroxidase, and oxidase activities in BpKatG and its variants

	Catalase	Peroxidase	Oxidase$_{(340)}$	Oxidase$_{(560)}$	Hydrazinolysis
			units/mg		
BpKatG	4100 ± 200	4.4 ± 0.5	6.9 ± 1.0	7.7 ± 1.2	0.9 ± 0.02
R108A	1250 ± 110	1.0 ± 0.1	3.7 ± 0.5	2.2 ± 0.4	0.3 ± 0.01
R108K	320 ± 20	0.9 ± 0.1	2.2 ± 0.2	1.3 ± 0.1	0.32 ± 0.01
H112A	1 ± 0.2	0.1 ± 0.01	ND[a]	ND	ND
H112N	2 ± 0.6	0.1 ± 0.01	3.1 ± 0.2	1.3 ± 0.5	0.2 ± 0.06
W111F	2 ± 0.1	3.3 ± 0.6	7.7 ± 2.4	ND	0.5 ± 0.04
D141A	60 ± 10	5.8 ± 0.4	2.2 ± 0.1	0.7 ± 0.1	0.5 ± 0.1
D141N	390 ± 20	5.4 ± 0.3	2.8 ± 0.2	1.2 ± 0.2	0.6 ± 0.1
D141E	3290 ± 40	6.3 ± 1.7	3.4 ± 0.1	2.8 ± 0.2	0.8 ± 0.02
Y238A	2 ± 0.1	6.1 ± 0.1	10.8 ± 1.9	0.4 ± 0.1	0.5 ± 0.04
Y238F	6 ± 1.1	2.8 ± 0.3	10.3 ± 2.0	ND	1.1 ± 0.05
M264A	6 ± 1.1	7.0 ± 1.4	4.3 ± 0.1	ND	0.6 ± 0.04
M264L	2 ± 0.9	6.1 ± 1.3	11.0 ± 1.5	4.9 ± 0.6	0.6 ± 0.04
MtKatG	3550 ± 160	9.7 ± 0.2	2.4 ± 0.8	1.2 ± 0.2	1.0 ± 0.06
EcKatG	2320 ± 230	9.9 ± 0.3	1.1 ± 0.4	0.2 ± 0.05	0.5 ± 0.02

[a] ND, not determined.

oxidase reaction was affected in several of the variants, and two groups with different properties can be discerned. One group, including those with changes in any of the three residues in the cross-linked structure of Trp^{111}, Tyr^{238}, and Met^{264}, exhibits normal rates of NADH disappearance but significantly reduced rates of radical production. The apparent uncoupling of NADH oxidation from superoxide generation could be a result of a broken electron tunnel or of a change in the reaction chemistry to favor H_2O_2 over superoxide formation. Unfortunately, the unambiguous identification or quantification of H_2O_2 formed in the reaction is not possible because it is immediately utilized in a peroxidatic reaction. Indeed, an inconclusive 13% hypochromic and 3–5-nm red shift in the Soret band and little change in the 500–700 nm region are observed for the W111F and Y238F variants during the oxidase reaction, whereas no change is observed with native BpKatG. The second group exhibits reduced rates of both NADH disappearance and superoxide formation, consistent with reduced NADH oxidation. This group includes those with changes in the active site residues Arg^{108}, His^{112}, and Asp^{141}. The changes in catalase and peroxidase activities caused by the sequence changes are consistent with those reported previously for KatGs from *Synechocystis* (38, 40, 41), *M. tuberculosis* (39), and *E. coli* (42).

Location of Conserved Residues—Because the *in vivo* peroxidase substrate remains unidentified, possible substrate-binding sites for as yet unidentified substrates was a topic for speculation in the original report of the BpKatG structure (44). Unambiguous identification of such sites will have to await a crystal structure determination of protein-ligand complexes, but further evidence for a diversity of binding sites in KatGs is shown in the high frequency of highly conserved residues (Table VI) and their broad distribution throughout the subunit including on the surface (Fig. 7). Over 27 and 18% of the residues, respectively, in the catalytic N-terminal domain and noncatalytic C-terminal domain of the KatG subunit are identical in more than 95% of the sequences. This is compared with the 8–14% frequency of nearly identical residues, all located near the active sites in pyruvate kinases, catalases, peroxidases, CuZn SODs, and FeMn SODs (data not shown).

DISCUSSION

The existence of catalase, peroxidase, and oxidase activities in a single protein makes KatG a complex and fascinating enzyme, an assessment further enhanced by INH hydrazinolysis and isonicotinoyl-NAD synthesis activities. A summary of these various activities (Fig. 8) illustrates the independence of the closely related catalase and peroxidase activities from the oxidase, hydrazinolysis, and synthase activities. Not only are

TABLE VI
Comparison of the percentage of highly conserved residues (>95% identical) in KatGs compared to other families of proteins

	KatG		Catalase	SOD		Peroxidase	Pyruvate kinase
	N-terminal	C-terminal		CuZn	FeMn		
No. in family	52[a]	52[a]	228[a]	22[b]	25[c]	24[d]	28[e]
Length	390	322	490	155	238	294	470
No. with >95% identity	107	59	57	22	22	24	59
Percentage with >95% identity	27.4	18.3	11.6	14.2	9.2	8.2	12.3

[a] Accession numbers are described by Klotz and Loewen (37).
[b] The accession numbers for the sequences used are: AA054860, AAR15417, AB087845, AF312586, AF312588, AF318938, AJ581746, AY428604, AY434497, BAC96317, BC061861, CAC28938, Jo2658, J04087, L13778, M15175, M84013, NM011435, NM174615, NP012638, NP231223, NP940620, P24704, X97766, and XM358882.
[c] The accession numbers for the sequences used are: AAN16456, AA057908, AB093035, AB109302, AF318020, AY314980, J03511, L11707, L25675, M33119, M60401, M74242, M94879, M96560, NM013671, NM057577, NM059889, NP011872, NP231679, NP232322, NP704405, NP940564, Q8K6Y8, and X03951.
[d] The accession numbers for the sequences used are: AB027752, AB009084, AB022273, AB024437, AB027752, AB027753, AF039027, AF109123, AF139910, AF149278, AF155124, AF159380, AF159629, AF175710, AJ003141, AJ011939, D11102, D11337, D14442, D83669, D84400, D90115, M60729, Y16773, and Y17192.
[e] The accession numbers for the sequences used are: AAB47952, AAH16619, AAH19265, AAHY25737, AAH61541, AAO57788, AAQ57928, BAC91436, BAD01636, CAA24631, CAE07913, CAE14987, CAE20854, NP230139, NP231642, NP416191, NP416368, NP703926, NP721573, NP881869, NP934082, NP939895, Q8Z6K2, Q9Z9B4, Q89AI8, XP224416, XP341924, ZP00026409, ZP00078743, and ZP000122573.

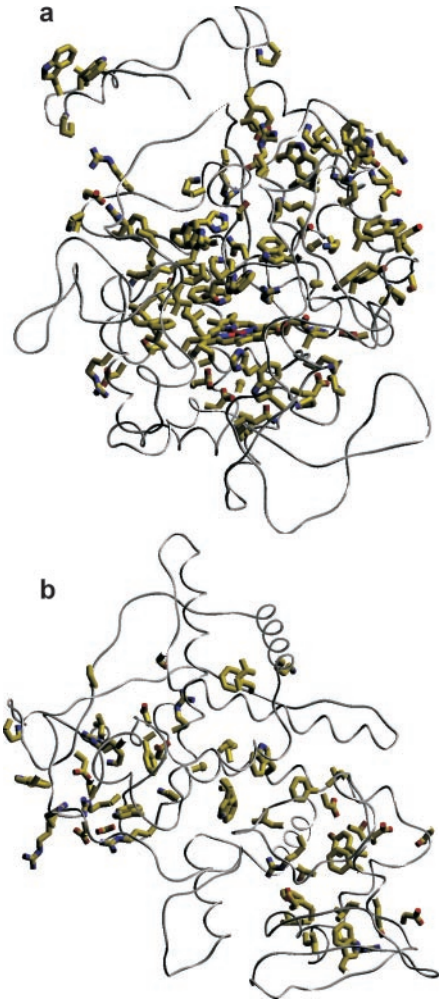

FIG. 7. **Location of residues in BpKatG that are identical in more than 95% of the 53 catalase-peroxidase sequences available.** The distribution in the N-terminal domain is shown in *a*, and the distribution in the C-terminal domain is shown in *b*. The domains are treated separately for a clearer representation of the differences.

the pH optima very different, but, unlike the catalase and peroxidase reactions, the oxidase, hydrazinolysis, and synthase reactions do not require H_2O_2 or involve the formation of identifiable oxidized heme intermediates. The hydrazinolysis and synthase reactions are closely linked because hydrazinolysis must occur before the ligation of NAD^+ to the isonicotinoyl radical, but the oxidase reaction is not mechanistically linked to any other reaction except that it very likely shares with the synthase the same NAD^+/NADH-binding site. In addition the oxidase reaction may serve as a source of NAD^+ for the synthase reaction and H_2O_2 for the catalase and peroxidase reactions (Fig. 8).

The catalase and peroxidase functions of KatG are rationalized as protection against H_2O_2, and the NADH oxidase activity may present a complementary protection against molecular oxygen or a means of maintaining low cytoplasmic levels of oxygen. However, the turnover rate of the oxidase is very slow compared with the catalase and peroxidase reactions, and the oxidase activity may simply be a residual vestige of what was once a more substantial activity with metabolic significance in a particular environmental niche. Certainly, the high affinity of the enzyme for NADH is consistent with there being, or having been, a physiological significance to the activity, and even among the three KatGs in this study, the variation in oxidase activity, highest in BpKatG and lower in MtKatG and EcKatG, might be interpreted as the result of an environmentally determined differential loss of activity.

Although the KatGs can utilize NADH as a peroxidatic substrate, the NADH oxidase characterized here is clearly not a peroxidatic reaction, and it is also different in several key respects from the peroxidase-oxidase activity associated with HRP. H_2O_2 does not have a catalytic role, SOD and catalase do not inhibit the reaction, and lag periods in reaction initiation are not evident in the presence of high enzyme or low NADH concentrations. In addition, the pH dependence of superoxide radical formation in the oxidase reaction suggests the unusual possibility of two reaction outcomes for molecular oxygen depending on proton availability. Below pH 8, with protons more readily available, a two electron transfer to oxygen takes place generating H_2O_2 (Reaction 1), whereas at higher pH, two one-electron transfers to two oxygen molecules generate two superoxide ions (Reaction 2). The protonation state of the imidazole ring of the distal side His^{112} may determine the reaction pathway through presentation of a proton to the bound oxygen in the active site. Any H_2O_2 produced via Reaction 1 would rapidly oxidize the heme to compound I and subsequent reduction in catalase or peroxidase reactions would give rise to H_2O.

$$NADH + O_2 + H^+ \rightarrow NAD^+ + H_2O_2$$

$$NADH + 2O_2 \rightarrow NAD^+ + 2O_2$$

REACTIONS 1 and 2

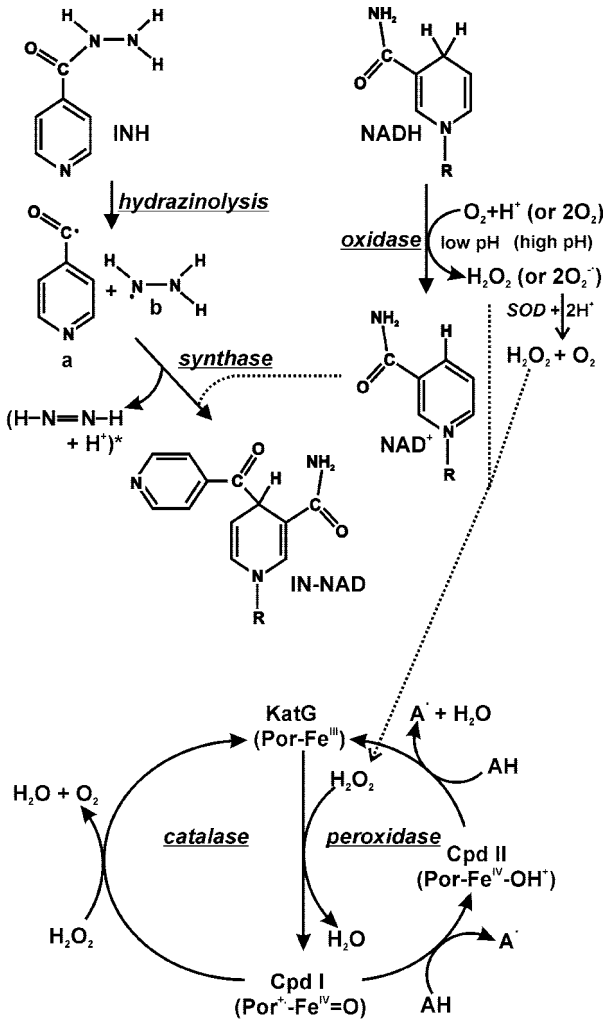

FIG. 8. **Scheme showing the relationship of the five activities of KatG.** The locations of the INH hydrazinolysis, NADH oxidase, isonicotinoyl-NAD synthase, catalase, and peroxidase reactions are *underlined*. The two pH-dependent options for the NADH oxidase reaction are also indicated. The isonicotinoyl (*a*) and hydrazide (*b*) radicals from the hydrazinolysis reaction are available to radical scavengers in the absence of NAD^+. The di-imide and proton products from the synthase reaction, indicated in *parentheses* with an *asterisk*, have not been confirmed as products but provide a convenient and logical way to balance the reaction. The catalase and peroxidase cycles are shown at the *bottom* and appear to be independent of the reactions at the *top* except for the possible metabolism of H_2O_2 generated in the oxidase reaction (*dotted line*) and the possibility that molecular oxygen may also bind to the heme.

The enhancement of INH hydrazinolysis by KatG and its importance in INH pro-drug activation is well documented. A single mutation in Ser^{315} of MtKatG is sufficient to reduce the affinity of the enzyme for INH (39) and to prevent isonicotinoyl-NAD formation (45) leading to *in vivo* isoniazid resistance. The facts that NAD^+ is a competitive inhibitor of NADH oxidation but does not inhibit the hydrazinolysis reaction and that an INH-NADH mixture supports a rate of radical production greater than the cumulative rates of the individual reactions suggest that NADH/NAD^+ and INH have separate binding sites and that there is an element of synergy between the two reactions. Manganese ions (both Mn^{+2} and Mn^{+3}) enhance both nonenzymatic and enzymatic hydrazinolysis to the extent that manganese-mediated isonicotinoyl radical formation is faster than the KatG-mediated reaction. However, despite this high rate of manganese-mediated hydrazinolysis, manganese-mediated isonicotinoyl-NAD formation is negligible compared with its rapid formation in the presence of KatG. The data in this report do not dispute the observation that there can be a nonenzymatic origin of isonicotinoyl-NAD (7), but under the conditions employed in this work, KatG is a much more effective catalyst of isonicotinoyl-NAD synthesis than manganese ion.

The regulatory systems controlling KatG expression, involving OxyR in *E. coli*, are generally oxidative response systems, supporting the conjecture that the primary role of KatG is the detoxification of H_2O_2 as a catalase. The physiological role and importance of the peroxidatic reaction in the anti-oxidant process remains unclear, in large part because the identity of the *in vivo* peroxidatic substrate(s) remains unknown. The wide variety of *in vitro* substrates that are utilized by KatG and the wide variety of substrates used by the closely related plant peroxidases, ranging from whole proteins to simple carbohydrates and metal ions, have not helped in the identification. Furthermore, the structure of KatGs present several potential substrate-binding sites in its surface topography, and there is an abnormally high percentage of highly conserved residues close to the protein surface, consistent with the idea of important features residing in other than the heme pocket. Of the known substrates, H_2O_2 binds at the heme iron, which is also the most likely site for O_2 binding; INH binds in the heme cavity or entrance channel near Ser^{324}; and the peroxidatic substrates probably also bind in the vicinity of Ser^{324} as suggested by benzhydroxamic acid binding in HRP (46), although the substrates used here are larger and would not fit into as small a cavity as benzhydroxamic acid. Trying to identify the NADH-binding site would be pure conjecture at this point, but the possibility that the cross-linked side chains of Trp^{111}, Tyr^{238}, and Met^{264} may have a role in electron transfer from NADH to O_2, and the observations that INH does not inhibit NADH oxidation and NAD^+ does not inhibit hydrazinolysis suggest that the NADH-binding site is some distance from the heme pocket. However, this surmise must be tempered by the logic of having NAD^+ bind in close proximity to the site of isonicotinoyl radical formation. A structural definition of the binding sites is needed.

Acknowledgments—The cooperation of Drs. K. G. Standing and W. Ens in arranging use of the mass spectrometers in the TOF Laboratory (supported by National Institutes of Health Grant GM59240) of the Department of Physics, University of Manitoba is also appreciated.

REFERENCES

1. Deretic, V., Pagan-Ramos, E., Zhang, Y., Dhandayuthapani, S., and Via, L. E. (1996) *Nat. Biotechnol.* **14,** 1557–1561
2. Zhang, Y., Heym, B. Allen, B., Young, D., and Cole, S. T. (1992) *Nature* **358,** 591–593
3. Johnsson, K., King, D. S., and Schultz, P. G. (1995) *J. Am. Chem. Soc.* **117,** 5009–5010
4. Rozwarski, D. A., Grant, G. A., Barton, D. H. R., Jacobs, W. R., and Sacchettini, J. C. (1998) *Science* **279,** 98–102
5. Mdluli, K., Slayden, R. A., Zhu, Y., Ramaswamy, S., Pan, X., Mead, D., Crane, D. D., Musser, J. M., and Barry, C. E. (1998) *Science* **280,** 1607–1610
6. Johnsson,. K., and Schultz, P. G. (1994) *J. Am. Chem. Soc.* **116,** 7425–7426
7. Wilming, M., and Johnsson, K. (1999) *Angew. Chem. Int. Ed.* **38,** 2588–2590
8. Magliozzo, R. S., and Marcinkeviciene, J. A. (1996) *J. Am. Chem. Soc.* **118,** 11303–11304
9. Lei, B., Wei, C. J., and Tu, S. C. (2000) *J. Biol. Chem.* **275,** 2520–2526
10. Minisci, F., Vismara, E., and Fontana, F. (1989) *Heterocycles* **28,** 489–519
11. Mitchison, D. A., and Selkon, J. B. (1956) *Am. Rev. Tuberc.* **74,** 109–116
12. Youatt, J. (1969) *Am. Rev. Respir. Dis.* **99,** 729–749
13. Wang, J. Y., Burger, R. M., and Drlica, K. (1998) *Antimicrob. Agents Chemother.* **42,** 709–711
14. Ashrafuddin, S., and Claiborne, A. (1989) *J. Biol. Chem.* **264,** 19856–19863
15. Zoldak, G., Sutak, R., Antalik, M. Sprinz, M., and Sedlak, E. (2003) *Eur. J. Biochem.* **270,** 4887–4897
16. Kengen, S. W. M., van der Oost, J., and de Vos, W. M. (2003) *Eur. J. Biochem.* **270,** 2885–2894
17. Xia, R., Webb, J. A., Gnall, L. L. M., Cutler, K., and Abramson, J. J. (2003) *Am. J. Physiol.* **285,** C215–C221
18. Akazawa, T., and Conn, E. E. (1958) *J. Biol. Chem.* **232,** 403–415
19. Yokota, K., and Yamazaki, I. (1965) *Biochim. Biophys. Acta* **105,** 301–312
20. Yokota, K., and Yamazaki, I. (1977) *Biochemistry* **16,** 1913–1920
21. Dunford, H. (1999) *Heme peroxidases*, Wiley-VCH, New York
22. Ro, Y. T., Lee, H. I., Kim, E. J., Koo, J. H., Kim, E., and Kim, Y. M. (2003) *FEMS Microbiol. Lett.* **226,** 397–403
23. Hillar, A., and Loewen, P. C. (1995) *Arch. Biochem. Biophys.* **323,** 438–446

24. Carpena, X., Switala, J., Loprasert, S., Mongkolsuk, S., Fita, I., and Loewen, P. C. (2002) *Acta Cryst.* **D58,** 2184–2186
25. Triggs-Raine, B. L., and Loewen, P. C. (1987) *Gene* **52,** 121–128
26. Loewen, P. C., Switala, J., Smolenski, M., and Triggs-Raine, B. L. (1990) *Biochem. Cell Biol.* **68,** 1037–1044
27. Rorth, H. M., and Jensen, P. K. (1967) *Biochim. Biophys. Acta* **139,** 171–173
28. Auclair, C., and Voisin, E. (1985) in *CRC Handbook of Methods for Oxygen Radical Research* (Greenwald, R. A., ed) pp. 123–132, CRC Press, Boca Raton, FL
29. Layne, E. (1957) *Methods Enzymol.* **3,** 447–454
30. Laemmli, U. K. (1970) *Nature* **227,** 680–685
31. Weber, K., Pringle, J. R., and Osborn, M. (1972) *Methods Enzymol.* **26,** 3–27
32. Davis, B. J. (1964) *Ann. N. Y. Acad. Sci.* **121,** 404–427
33. Gregory, E. M., and Fridovich, I. (1974) *Anal. Biochem.* **58,** 57–62
34. Clare, D. A., Duong, M. N., Darr, D., and Archibald, F. (1984) *Anal. Biochem.* **140,** 532–537
35. Loboda A. V., Krutchinsky, A. N., Bromirski, M., Ens, W., and Standing, K. G. (2000) *Rapid Commun. Mass Spectrom* **14,** 1047–1057
36. Thompson, J. D., Higgins, D. G., and Gibson, T. J. (1994) *Nucleic Acids Res.* **22,** 4673–4680
37. Klotz, M. G., and Loewen, P. C. (2003) *Mol. Biol. Evol.* **20,** 1098–1112
38. Jakopitsch, C. Auer, M., Ivancich, A., Ruker, F., Furtmuller, P. G., and Obinger, C. (2003) *J. Biol. Chem.* **278,** 20185–20191
39. Yu, S., Girotto, S., Zhao, X., and Magliozzo, R. S. (2003) *J. Biol. Chem.* **278,** 44121–44127
40. Jakopitsch, C. Auer, M., Regelsberger, G., Jantschko, W., Furtmuller, P. G., Ruker, F., and Obinger, C. (2003) *Biochemistry* **42,** 5292–5300
41. Regelsberger, G., Jakopitsch, C., Ruker, F., Krois, D., Peschek, G. A., and Obinger, C. (2000) *J. Biol. Chem.* **275,** 22854–22861
42. Hillar, A., Peters, B., Pauls, R., Loboda, A., Zhang, H., Mauk, A. G., and Loewen, P. C. (2000) *Biochemistry* **39,** 5868–5875
43. Yamada, Y., Fujiwara, T., Sato, T., Igarashi, N., and Tanaka, N. (2002) *Nat. Struct. Biol.* **9,** 691–695
44. Carpena, X., Loprasert, S., Mongkolsuk, S., Switala, J., Loewen, P. C., and Fita, I. (2003) *J. Mol. Biol.* **327,** 475–489
45. Wei, C. J., Lei, B., Musser, J. M., and Tu, S. C. (2003) *Antimicrob. Agents Chemother.* **47,** 670–675
46. Henriksen, A., Schuller, D. J., Meno, K., Welinder, K. G., Smith, A. T., and Gajhede, M. (1998) *Biochemistry* **37,** 8054–8060